HHS Public Access

Author manuscript

*Ann Biomed Eng*. Author manuscript; available in PMC 2018 February 01.

Published in final edited form as:

*Ann Biomed Eng*. 2017 February ; 45(2): 452–463. doi:10.1007/s10439-016-1618-2.

# Hemodynamic Performance and Thrombogenic Properties of a Superhydrophobic Bileaflet Mechanical Heart Valve

**David L. Bark Jr.**[1,2], **Hamed Vahabi**[1], **Hieu Bui**[2], **Sanli Movafaghi**[1], **Brandon Moore**[1], **Arun K. Kota**[1,2], **Ketul Popat**[1,2], and **Lakshmi P. Dasi**[+,1,2]

[1]Colorado State University, Department of Mechanical Engineering, Fort Collins, CO, United States

[2]Colorado State University, School of Biomedical Engineering, Fort Collins, CO, United States

## Abstract

In this study, we explore how blood-material interactions and hemodynamics are impacted by rendering a clinical quality 25 mm St. Jude Medical Bileaflet mechanical heart valve (BMHV) superhydrophobic (SH) with the aim of reducing thrombo-embolic complications associated with BMHVs. Basic cell adhesion is evaluated to assess blood-material interactions, while hemodynamic performance is analyzed with and without the SH coating. Results show that a SH coating with a receding contact angle (CA) of 160º strikingly eliminates platelet and leukocyte adhesion to the surface. Alternatively, many platelets attach to and activate on pyrolytic carbon (receding CA=47), the base material for BMHVs. We further show that the performance index increases by 2.5% for coated valve relative to an uncoated valve, with a maximum possible improved performance of 5%. Both valves exhibit instantaneous shear stress below 10 N/m$^2$ and Reynolds Shear Stress below 100 N/m$^2$. Therefore, a SH BMHV has the potential to relax the requirement for antiplatelet and anticoagulant drug regimens typically required for patients receiving MHVs by minimizing blood-material interactions, while having a minimal impact on hemodynamics. We show for the first time that SH-coated surfaces may be a promising direction to minimize thrombotic complications in complex devices such as heart valves.

### Keywords

shear stress; superhydrophobic; thrombosis; turbulence; blood; bileaflet mechanical heart valve

## Introduction

Hundreds of thousands failing heart valves are replaced with bioprosthetic or mechanical valves each year as a result of valvular disease [60, 86]. Bioprosthetic valves suffer from durability issues and are at high risk for structural deterioration in children [71, 78]. Therefore, patients receiving these valves require reoperative procedures, increasing the risk for adverse events [16, 43]. Alternatively, mechanical heart valves (MHV)s are at risk for thromboembolism due to non-phsyiological hemodynamics and through blood-material

[+]Correspondence to: Department of Biomedical Engineering, Dorothy Davis Heart and Lung Research Institute 473 W 12th Avenue, Columbus, OH 43210, USA.

reactivity [4, 5, 13, 15, 40, 79]. To mitigate risks, patients are treated with systemic lifelong anticoagulant/antiplatelet drug regimens, which increases the bleeding risk, restricts lifestyle, and can even cause death [58, 74]. These drawbacks have resulted in a drop in patients receiving MHVs [11, 33]. However, if these durable valves are made with thrombo-resistant materials and/or if non-physiological hemodynamics are impacted, then less aggressive anticoagulant and antiplatelet therapies would be required.

One concern with MHVs is the potential for hemolysis (erythrocyte rupture) and platelet activation associated with non-physiologically high shear stress [8, 9, 38, 59, 87, 88]. Hemolysis can have many detrimental effects, including anemia in extreme cases [81]. In all cases of rupture, erythrocytes release adenosine diphosphate, a platelet activation agonist that can promote thrombosis [19, 20]. Shear stress can also directly stimulate platelet activation in the absence of hemolysis, further promoting thrombo-embolic complications [1, 3, 8, 9, 38]. As a result of these risks, many studies have attempted to characterize shear stress and Reynolds shear stress (RSS) in MHVs through experimental and computational fluid dynamics [25, 34, 55, 76, 87]. Sotiropoulos et al. provides a review of these dynamics and an explanation for how RSS can contribute to hemolysis or platelet activation by impacting the instantaneous shear stress experienced by blood cells is further explored in Morshed et al. [59, 76]. Generally, these studies of RSS and shear stress find that stresses downstream of the bileaflet St. Jude valve remain below values that should induce hemolysis for MHVs. However, temporal fluctuations in stress, leakage through the valve, hinge regions of the valve, and foreign surfaces complicate the situation [6, 28, 34, 88]. The impact of MHV hemodynamics on thrombosis remains poorly defined since platelet activation is time-dependent, involves complex signaling with feedforward chemical pathways, and since activation can be reversible [30, 36, 38, 39, 90]. Despite these complications, there have been attempts to incorporate these parameters into blood damage accumulation models [2, 9, 38, 62]. Combined, these studies indicate that a reduction of instantaneous shear stress may lower the potential for blood damage.

In addition to adverse hemodynamics, blood-material interactions can result in thrombosis [7, 10]. For example, various synthetic valves have been designed to exhibit similar hemodynamics to bioprosthetic and native heart valves, yet they still suffer from thrombotic complications [22, 35, 84, 85]. Therefore, various material treatments have been developed in attempts to mitigate this risk [7, 41]. One approach is to weaken the interaction of cell and protein adhesion to a surface by using hydrophilic surfaces or through the application of an unreactive protein to the surface [42, 44, 51, 66]. However, hydrophilic polymers, such as polyethylene oxide or polyethylene glycol are known to decompose over time as a result of oxidation [21]. Furthermore, macrophages can adhere to unreactive proteins like albumin, stimulating an inflammatory response [37]. A second approach is to inhibit the various pathways involved in thrombosis through the release of agents such as heparin [18, 27, 73, 82]. However, there are often leaching issues with this method, degrading the thrombo-resistive properties of the surface over time [18]. Overall, despite efforts, many of these materials have only exhibited marginal benefits in clinical studies [49, 68].

Superhydrophobic (SH) surfaces, i.e. surfaces that are extremely repellent to water, may provide an alternative approach to minimize the thrombotic risk associated with blood-

material interactions [45, 53, 80]. These surfaces, exemplified by the lotus leaf in nature, are fabricated by combining materials with low solid surface energy (typically $\gamma_{sv} < 15$ mN $m^{-1}$) and texture [46–48]. Low solid surface energy makes the surface hydrophobic and is controlled by chemical composition through functional groups, such as $–CF_3$. The primary measure of wetting of a liquid on these non-textured (i.e., smooth) surfaces is the equilibrium (or Young's) contact angle $\theta$ [89]. Materials with a low solid surface energy can reach contact angles as high as 120° [61]. Furthermore, these surfaces are known to promote plasma protein adhesion and can impact plasma protein conformation [57, 69]. Superhydrophobicity can be created by adding texture to surfaces with low solid surface energy, with enhanced effects seen for hierarchical texture involving microscale and nanoscale structures. When a liquid droplet contacts a textured (i.e., rough) solid surface, it displays an apparent contact angle $\theta^*$, and it can adopt one two configurations to minimize its overall free energy – the fully wetted Wenzel state or the partially wetted Cassie-Baxter state [14, 83]. Microscopic pockets of air exist in the texture of the Cassie-Baxter state, which leads to a composite liquid-air-solid interface and thus minimizes the solid-liquid interface. The Cassie-Baxter state leads to high $\theta^*$ and low contact angle hysteresis $\Delta\theta^*$ [14]. A surface is considered SH if it displays $\theta^* > 150°$ and $\Delta\theta^* < 10°$ with water [46, 47]. In addition to minimizing blood-material reactions, surfaces based on the Cassie and Baxter state may alter local hemodynamics since fluid slip can exist along the surface, potentially reducing the risk for hemolysis and shear-induced platelet activation [17, 50, 64, 65, 70, 77]. Here, we are interested in evaluating the potential use of SH surfaces as a MHVs leaflet material with the aim of reducing the thrombogenic properties of current pyrolytic carbon-based valve leaflets. This study only explores the SH paradigm, while additional work will be needed to optimize the durability of the SH surface and to further assess the thrombotic potential of a SH valve in a physiological blood flow environment.

## Materials and Methods

### Superhydrophobic Coating on a Mechanical Bileaflet Heart Valve

Ultra-Ever Dry (UltraTech International, Inc., Jacksonville, FL) is a commercially available SH coating used in this study. The coating involves a bottom layer of coarser texture and a top layer of finer texture. A combination of the coarser and finer scale texture results in a hierarchical structure that increases the hydrophobicity relative to a single length scale structure. The hierarchical texture was applied as a spray to a 25 mm St. Jude Medical™ standard pyrolytic carbon (PyC) bileaflet mechanical heart valve (BMHV), using an airbrush (Paasche Airbrush Company, Chicago, IL) with a spray pressure of 30 psi. For this procedure, glass or PyC was exposed to oxygen plasma for 15 minutes to enhance the adhesiveness of the coating. The bottom coating of coarser texture was allowed to dry for 5 minutes prior to spraying the top coating, which was allowed to dry for 15 minutes. Both coatings dried at room temperature. The presence of the coating was tested through contact angle measurements. The BMHV was used for hemodynamic/hydrodynamic experiments. Due to limitations in obtaining PyC samples, we also applied a coarse and hierarchical texture to glass for blood studies. This becomes necessary to compare various surface treatments for a given sample of blood. With a sufficient coating thickness, the base material should not contact the blood, whether PyC or glass, as further described in the

supplementary material. In this work, we denote surfaces with the coarse layer only as "coarse", while surfaces with the coarse and fine layer are labeled as "hierarchical", followed by the type of base material.

## Characterization of Surface Hydrophobicity

Advancing and receding contact angles (CA)s were used to assess the hydrophobicity through a Rame-Hart goniometer. Reported CAs were measured between the solid-liquid and liquid-vapor interfaces of a small (8–12 μL) droplet of deionized water placed on a surface of interest. CA hysteresis is reported as the difference in advancing and receding CAs. Roll-off angles were also measured by applying a 8–12 μL water droplet to the surface. For this test, the surface was tilted at an angle relative to the horizontal until the droplet rolled or slid.

Additional tests were performed to demonstrate the repellence of surfaces to blood. In the first test, we dropped 12 μl of blood onto surfaces from a height of 10 mm to observe potential bouncing. In a second test, a 30 μl droplet of blood was placed along various surfaces at a 45º angle. The increased volume was used to make the blood droplet slide along the glass surface. A FASTCAM SA3 high speed camera (Photron, Inc.) was used to capture videos for both tests at 1500 frames per second.

## Blood-Material Reactivity

As a preliminary assessment of hemocompatiblity, we compared platelet and leukocyte adhesion on glass, PyC, coarse glass, and hierarchical glass. Human blood was drawn through venipuncture from healthy individuals, who stated that they were free of anticoagulant or antiplatelet medications, such as aspirin for at least 10 days. All blood donors provided written consent for the study in accordance with the Internal Review Board of Colorado State University. Plasma was isolated from erythrocytes by centrifuging the blood anticoagulated with ethylenediaminetetraacetic acid (EDTA) at 100 g for 15 minutes. 2 ml of pooled plasma was subsequently incubated with each sample in a 12-well plate. Incubation was performed at room temperature on a horizontal shaker plate (100 revolutions per minute) for 2 hours with the aim of dispersing coagulation factors produced from activating platelets. These methods are similar to previously used techniques to assess platelet adhesion and activation on various biomaterials [23, 52, 53, 63, 75]. After incubation, samples were fixed with 1% gluteraldehyde and were dried through a series of ethanol treatments. Samples were then imaged using scanning electron microcopy to determine the amount of cell adhesion.

## Steady Flow Hemodynamic Performance

To quantify the energy loss across the coated valve relative to an uncoated valve, we calculated the effective orifice area (EOA) based on the ISO-5840/2005 guidance document. In this document, the EOA is defined as:

$$A_{EO} = \frac{Q_{rms}}{51.6\sqrt{\Delta P/\rho}}, \quad \text{Eq. 1}$$

where $Q_{rms}$ is the root mean square of forward flow in ml/s, $\Delta P$ is the mean pressure difference across the valve in mmHg, and $\rho$ is the density of the fluid in g/cm$^3$. Pressure was measured with a manometer one diameter upstream and three diameters downstream of the valve in a specially designed chamber with an internal diameter of 35 mm. Flow rates were also measured using an ultrasonic flow probe (Transonic Inc., Ithaca, NY). The flow system is shown in Fig. 1A. To calculate the EOA (Eq. 1), steady flow was supplied to the valve using a submersible pump (G535AG20 Beckett Corporation, Irving, TX) to control flow rates from 5 to 30 l/min with 5 l/min intervals. Flow rates were controlled by providing flow resistance through a ball valve in-line with the prosthetic heart valve. Experiments were repeated 3 times. A line crossing zero was fit through the data with flow rate plotted against the square root of the pressure drop. After a unit conversion, the slope was reported as the effective orifice area. The fluid used for this test involved a glycerin and water mixture with viscosity of 3.6 cP and density of 1000 kg/m$^3$.

Performance was also evaluated by calculating the Performance Index (PI), defined as the effective orifice area normalized with the geometrical annulus area. In this study, the annulus area is defined as the cross sectional thickness of each leaflet subtracted from the housing internal orifice area. The coating changes this area as it adds thickness to the leaflets and decreases the housing orifice area. Coating thickness was estimated via inspection of its cross section using the optical microscope.

### Pulsatile Flow Hemodynamic Performance Through Particle Imaging Velocimetry

Physiological pulsatile flow was established using ISO 5840/2005 in a left heart simulator previously described in Ref [32] and is shown in Fig. 1B for particle imaging velocimetry (PIV) experiments. The flow loop was driven by a custom fabricated bladder pump, controlled by air pressure and solenoid valves through a custom LabView (National Instruments Corporation, Austin, TX) program. Pressure transducers (ValiDyne Engineering, Northridge, CA) were also placed upstream and downstream of valve fixed in a mounting chamber in-line with an ultrasonic flow probe. A compliance chamber and a resistance valve were placed downstream of the mounting chamber. Air pressure to the bladder pump, compliance, and the resistance were adjusted to obtain a systolic/diastolic pressure ratio of 120/80 mmHg, a cardiac output of 5 L/min, and a pulsatile rate of 60 beats per minute with a systolic duration of 35%. These values were maintained within 10% throughout the experiment.

We used PIV to quantify the flow field on the downstream side of the testing valve. PIV was performed in a phase-locked mode to capture peak flow corresponding to normal physiological aortic conditions described above. A glycerin and water mixture at viscosity of 3.6 cP and density of 1000 kg/m$^3$ was seeded with 1–20 μm melamine resin particles coated with Rhodamine-B. A Nd:YLF Single Cavity Diode Pumped Solid State High Repetition Rate Laser (Photonics Industries, Bohemia, NY) was used to illuminate a 0.2 mm thick measurement plane. The measurement plane was imaged with a double frame FASTCAM SA3 high speed camera. DaVis (Lavision, Inc.) was used to post-process PIV slices using an ensemble of approximately 250 phase-locked measurements. Turbulence was characterized using the 2D RSS, obtained through Reynolds decomposition, calculated as:

$$\rho\overline{u'v'} = \rho\frac{1}{N}\sum_{i=1}^{N} u_i' v_i', \quad \text{Eq. 2}$$

where *u'* and v' are the fluctuating velocities in the *x* (streamwise) and *y* direction respectively. N is the number of cycles, which was 250. The RSS is not a physical stress experienced by the cells [34, 59]. However, the value is reported for relative comparison with the literature and since it still provides predictive capability for blood damage. Therefore, we also calculated the instantaneous shear stress to assess the potential for hemodynamic stress-induced blood damage using:

$$\tau_{xy} = \mu\left(\frac{\partial u}{\partial y} + \frac{\partial v}{\partial x}\right), \quad \text{Eq. 3}$$

where $\mu$ is the dynamic viscosity. Shear stress was computed using a central differencing scheme, preceded by a 3x3 Gaussian filter, as previously used in Ge et al.[34].

### Computational Fluid Dynamics

ANSYS Fluent (Canonsburg, PA) was used to compare the pressure drop of a standard bileaflet mechanical heart valve (BMHV), with an idealized SH BMHV. For this purpose, a no-slip condition was applied as a boundary condition at the surface for the BMHV, while a second simulation was performed with free-slip along the SH BMHV surface. A free-slip condition was chosen because SH surfaces can exhibit varying degrees of fluid-slip along the surface [24, 56]. A free-slip condition provides an extreme case, counter to the no-slip condition. An improvement in hemodynamics for a free-slip condition warrants further optimization of the surface from a hemodynamics perspective; whereas minimal change would indicate that valve design may have more impact on hemodynamics through form drag experienced by the valve. Valve geometries were identical and were created to mimic the experimental valves in the open configuration. Leaflet positions remained fixed during the simulation. Simulations involved an unstructured three-dimensional grid (~1.8 million cells) with a half-sine wave velocity boundary condition at the inlet from 0 to 1 m/s, corresponding to a flow rate of 0 to 30 l/min. Specified flow rates are typical of flow through the aortic valve. A 0 pressure condition was applied as the outlet boundary. Out-of-plane vorticity was calculated using:

$$\omega_z = \frac{\partial v}{\partial x} - \frac{\partial u}{\partial y}. \quad \text{Eq. 3}$$

## Results

Results are organized with an initial quantification of hydrophobicity. Blood-material reactivity is then assessed based on cell adhesion. Subsequently, hemodynamics are characterized to investigate the potential for blood damage due to fluid stress using steady

and pulsatile flow experiments. These results are finally compared with computational results of an idealized valve.

## Characterization of Surface Hydrophobicity

PyC with a hierarchical coating repels water and blood, as demonstrated by the beading of both fluids, Fig. 2A, B. The contact angles of water are reported in Table 1. These results demonstrate that PyC changes from a slightly hydrophilic surface with a receding contact angle of 47º to a superhydrophobic surface with a receding contact angle of 160º after the hierarchical coating. Alternatively, the coarse coating maintains a receding contact angle of 70º. Furthermore, with a hierarchical coating, the contact angle hysteresis is only 4º. With these properties, blood bounces off of the hierarchical surface, while it sticks to PyC, as demonstrated in Fig. 2C and supplementary video 1.

The movement of blood is also visualized by placing a 30 μl droplet of blood on various surfaces tilted at 45º relative to the horizontal. Results are shown in Fig. 2D and supplementary video 2. The droplet slowly slides down a surface of bare glass and PyC, leaving a trail of blood. No movement is observed on glass coated with a coarse texture. Conversley, a droplet of blood swiftly slides off of a hierarchical glass slide, leaving no visual trace of blood on the surface. The roll-off angles (minimum angle by which a surface should be tilted relative to the horizontal for a droplet to roll off) for water are listed in Table 1. A water droplet rolls or slides off of the glass coated with a hierarchical texture when the surface is tilted by 5º or more, relative to the horizontal. Water does not roll or slide off of any other surface, even at a 90º tilt angle (i.e. surface is vertical). These results demonstrate that the hierarchical coating renders the surface SH.

## Blood-Material Reactivity

A preliminary assessment of the blood-material thrombotic response is performed by evaluating platelet and leukocyte adhesion. Glass and PyC result in substantial platelet adhesion, as shown in Fig. 3. Furthermore, adherent platelets exhibit sphering of the platelet body and multiple filopodia projections, demonstrating activation. Even more platelet adhesion can be seen on the coarse coating. This surface also results in the adhesion of multiple leukocytes, unlike the other surfaces. However, strikingly, no leukocytes or platelets are seen on the hierarchical coating, which involves a microscale (top row) and a nanoscale (bottom row) structure that can be seen in Fig. 3. Overall, the SH hierarchical coating strikingly eliminated the adhesion of leukocytes or platelets to the surface, while substantial adhesion is seen on other surfaces.

## Effective Orifice Area

A SH coating could alter hemodynamic performance by creating fluid slip along the surface. Therefore, the effective orifice area (EOA) of the valve is tested with and without the hierarchical coating. The EOA of the 25 mm PyC BMHV is 3.78 ± 0.15 $cm^2$ ($R^2$=0.998), which decreases to 3.45 ± 0.07 $cm^2$ ($R^2$=0.998) with the hierarchical coating. The performance index (PI) is also calculated since the 0.3 mm thick hierarchical coating decreases the geometric orifice area. As opposed the EOA, the PI increases from 0.77 ± 0.03

for to 0.79 ± 0.02 for the hierarchical coated valve, demonstrating a 2.5% improved performance if both valves exhibited the same geometric orifice area.

### Pulsatile Flow Experiments - Particle Imaging Velocimetry

Potential slip along the hierarchical coated PyC surface could alter the flow field downstream of the valve under pulsatile flow conditions. To test this possibility, the PyC and hierachical BMHV are placed in a left heart simulator. Representative ensemble averaged flow and pressure curves are presented in Fig. 4A for these experiments. Only one set of curves are shown because these curves are within the variance of typical experimental results irrespective of the SH coating. PIV is performed on both valves during peak flow, labeled in Fig. 4A. The instantaneous shear stress for each valve is shown in Fig. 4B with values similar for both valves, remaining below 10 $N/m^2$. However, one notable difference between the two valves is that the instantaneous shear stress is higher in the sinus region of the coated valve relative to the uncoated valve, demonstrating less flow stagnation. Instantaneous shear stress only provides data for a single representative point in time and does not describe the statistical characteristics of turbulence. Therefore, RSS contours are also quantified in Fig. 4C. RSS remains below 100 $N/m^2$ and is higher near the leaflets of the thicker coated valve relative to the PyC BMHV. RSS is also high along the shear layer initiating form the valve housing for both valves. For this region, RSS remains relatively confined within the aortic sinus for the hierarchical coating, whereas RSS of the same order extends past the sinus for the PyC valve. Therefore, similar downstream hemodynamics are seen for both valves, with a small improvement for the BMHV with a hierarchical texture.

### Computational Fluid Dynamic Results

We are further interested in quantifying the optimal improved hemodynamic performance of the BMHV if there is free-slip along the leaflet surface. Improved performance in this context would correspond to a reduced pressure drop across the valve for a given flow rate. Computational fluid dynamics (CFD) is used to create idealized conditions involving no-slip and free-slip along the simulated leaflets. Fig. 5A shows the pressure drop across the valves as peak inlet flow rate is reached. The pressure drop across the valve at 30 L/min for a free-slip condition is 4.79 mmHg and is only marginally lower than the no-slip condition, which exhibits a pressure drop of 5.28 mmHg. Therefore, the corresponding EOA for the free-slip condition only improves by 5% over the no-slip condition. To investigate the pressure drop further, we evaluated vorticity, as shown in Fig. 5B. Supplementary video 3 compares the velocity field in the vicinity of the leaflets for the two cases. The free-slip valve exhibits slightly smaller vortex structures downstream of the valve relative to the no-slip condition during peak flow and during the deceleration phase, Fig 5B. Combined, these results show that downstream hemodynamics are improved for a valve with free-slip over a BMHV with no-slip, but the difference is only minor.

## Discussion

In this article we investigated the potential use of a SH coating in prosthetic heart valves with the aim of overcoming thrombosis, the major drawback of current MHVs. The coating was able to dramatically reduce blood cell adhesion in a static environment relative to bare

PyC, demonstrating a reduction in the risk for thrombosis based on blood-material interactions. Furthermore, the SH valve maintained a similar hemodynamic environment to PyC BMHVs, demonstrating no added hemodynamic damage to blood cells relative to approved prosthetic heart valves. Therefore, any thrombosis due to high shear stress and recirculation regions in MHV would still likely exist in a SH MHV, unless the valve design is modified. Therefore, additional flow control techniques can be employed, such as the use of vortex generators [26, 31].

Other SH surfaces including nanostructured polycarbonate urethane films and $CO_2$-pulsed laser-treated polydimethylsiloxane have also been shown to minimize blood cell adhesion [45, 80]. Similar results have been shown for static and flow conditions with tethered-liquid perfluorocarbon coatings that create a controlled liquid barrier between blood and the surface [53]. These additional studies support the potential for a thrombo-resistive SH treatment in a heart valve application, while also demonstrating multiple methods that can be used to render valves SH.

Contrary to a SH hierarchical coating, the coarse texture exhibited a marked increase in both platelet and leukocyte adhesion. A general increase in cell adhesion may be associated with the increased affinity of plasma protein adsorption or protein conformational changes affiliated with hydrophobic surfaces [57, 69]. Alternatively, it may be associated with the increased surface area resulting from the coarse texture. Furthermore, fluorinated coatings used to create SH surfaces are known to cause a conformational change in albumin such that it supports Mac-1 binding, an integrin found on leukocytes, providing a possible explanation for the enhanced leukocyte adhesion on the coarse texture [37]. Combined these results provide potential explanations for the enhanced cell binding, but the exact mechanisms involved are not fully defined.

The movement of blood by gravity along surfaces at a 45º tilt angle in Fig. 2 can be explained by the CAs and by CA hysteresis [29, 67]. During sliding or rolling, the leading edge of the blood droplet displays the advancing CA, while the trailing edge of the droplet displays the receding CA [29]. The very low receding CA and high hysteresis maintains the trail of blood behind the droplet on glass and PyC surfaces. If the CA hysteresis is sufficiently high, the drop will remain adherent [29]. This was seen with the coarse texture, which has the highest hysteresis among all evaluated surfaces, with a value of 46º. Conversely, if CA hysteresis is small, then the drop freely moves down the surface, as seen for the hierarchical coating on glass [67].

Non-physiological hemodynamics, specifically regions of stagnating flow and regions of high shear stress, can also induce a thrombotic response. Stagnating flow can occur in the aortic sinus downstream of the aortic valve [87]. Therefore, there is need to drive fluid out through washout to restrict the persistence of stagnating flow. A SH coating appeared to increase the washout relative to an uncoated valve, demonstrated by high instantaneous shear stress near the sinus wall.

As mentioned, regions of high shear stress can also cause a thrombotic response, specifically through hemolysis and shear-induced platelet activation. However, the values causing

hemolysis and platelet activation remain ill-defined due to variations in studies and due to a dependence on exposure time to a specific shear stress. For a conservative estimation, shear stress must be above 1500 dynes/cm$^2$ to cause hemolysis and above 100 dynes/cm$^2$ to cause platelet activation [34, 38]. Here, we show that instantaneous shear stress is below 100 dynes/cm$^2$ for both the PyC BMHV and the SH BMHV, with values similar to Ge et al. [34]. Turbulence can further complicate the fate of blood cells due to spatio-temporal fluctuations in shear stress. In the case of turbulence, RSS is commonly used to predict blood damage, despite the fact it is a statistical measure and not an actual stress experienced by blood cells [34, 59]. Here, we show that the RSS magnitude remains below 1000 dynes/cm$^2$ at peak flow, with values similar to Ge et al. [34]. This value is below 4000 dynes/cm$^2$, a value shown to support hemolysis [72]. Less is known about the response of platelets to turbulence. Also, we were unable to capture the flow field in the boundary layer of the valve leaflets. However, cells in this region should experience lower shear stress for a SH BMHV, due to the presence of slip along the surface [24, 56]. These results indicate that a coated BMHV is unlikely to cause blood damage due to downstream flow from the valve.

We initially hypothesized that a SH coating could reduce friction drag, therefore reducing the energy dissipation along the valve leaflets. This hypothesis is based on slip and drag reduction previously seen for SH surfaces in the Cassie-Baxter state [17, 50, 64, 65, 70, 77]. However, we only found a slight improvement for the SH BMHV relative to the PyC BMHV based on PI calculations. Even for idealized free-slip in CFD, we found minimal improvement in energy dissipation across the valve. Therefore, form drag likely dominates energy dissipation across the MHV in this study, while surface slip is unlikely to improve energy loss performance of the studied BMHV. In this case, dissipation is likely associated with the complex vorticity structures seen downstream of the valve. These structures are described in more detail elsewhere [25, 76, 87]. Other methods involving passive flow control may alter these structures and could be combined with SH technology to improve performance [12, 26, 31, 54].

The advantages to SH technology is not limited to BMHVs. Instead, it could be useful for numerous blood-contacting medical devices including other prosthetic heart valves, left ventricular assist devices, extracorporeal devices, and stents among others. Many of these devices also suffer from thrombosis caused by non-physiological hemodynamics and/or blood-material interactions.

## Limitations

This study is intended to be a preliminary assessment for the use of SH BMHVs. Therefore, we used a commercially available SH coating as opposed to a method tailored for BMHVs. Static blood studies were performed for an initial evaluation of blood-material interactions. However, blood may respond differently under flow, warranting future investigation. Additional studies will also need to be performed to investigate long term performance of the valve if it were implanted. Hemodynamic analyses in this study were 2D and were limited to downstream flow. Therefore, we could not fully evaluate the complex three-dimensional coherent structures in the valve and we did not capture flow in leakage gaps for a closed valve. Despite this limitation, we were able to demonstrate that the instantaneous

shear stress and the RSS are similar irrespective of a SH coating. In this regard, RSS calculations assume minimal cycle-to-cycle variation in leaflet kinematics, which can otherwise influence calculated turbulence parameters. For this reason, we chose to evaluate the RSS when the valve is fully open, as opposed to when it is in a transient state. Lastly, CFD was limited in spatial resolution, limiting its ability to capture small scale fluid structures. Despite these limitations, the results presented here indicate that a SH MHV may reduce the propensity for thrombo-embolic complications.

## Conclusions

A superhydrophobic coating on a bileaflet mechanical heart valve is found to dramatically reduce cell adhesion when put into contact with blood, indicating a reduction in thrombotic potential caused by blood-material interactions. Furthermore, the coating minimally impacts valve hemodynamics, therefore minimizing any increased blood cell damage due to fluid stress. These results indicate that a superhydrophobic prosthetic heart valve may reduce the thrombo-embolic potential of current approved mechanical heart valves.

## Supplementary Material

Refer to Web version on PubMed Central for supplementary material.

## Acknowledgments

The authors gratefully acknowledge funding from National Institutes of Health (NIH) under Award Number R01HL119824 and F32HL129730. The content is solely the responsibility of the authors and does not necessarily represent the official views of the NIH.

## References

1. Bark DL Jr, Ku DN. Platelet Transport Rates and Binding Kinetics at High Shear over a Thrombus. Biophys J. 2013; 105:502–511. [PubMed: 23870271]
2. Bark DL Jr, Ku DN. Wall shear over high degree stenoses pertinent to atherothrombosis. J Biomech. 2010; 43:2970–2977. [PubMed: 20728892]
3. Bark DL Jr, Para AN, Ku DN. Correlation of thrombosis growth rate to pathological wall shear rate during platelet accumulation. Biotechnol Bioeng. 2012; 109:2642–2650. [PubMed: 22539078]
4. Baudet E, Oca C, Roques X, Laborde M, Hafez A, Collot M, Ghidoni I. A 5 1/2 year experience with the St. Jude Medical cardiac valve prosthesis. Early and late results of 737 valve replacements in 671 patients. The Journal of thoracic and cardiovascular surgery. 1985; 90:137–144. [PubMed: 3874324]
5. Baudet EM, Puel V, McBride JT, Grimaud J-P, Roques F, Clerc F, Roques X, Laborde N. Long-term results of valve replacement with the St. Jude Medical prosthesis. The Journal of thoracic and cardiovascular surgery. 1995; 109:858–870. [PubMed: 7739245]
6. Bellofiore A, Quinlan NJ. High-Resolution Measurement of the Unsteady Velocity Field to Evaluate Blood Damage Induced by a Mechanical Heart Valve. Ann Biomed Eng. 2011; 39:2417–2429. [PubMed: 21638140]
7. Bezuidenhout, D., Zilla, P. Cardiovascular and Cardiac Therapeutic Devices. Springer; 2014. Flexible leaflet polymeric heart valves; p. 93-129.
8. Bluestein D, Niu L, Schoephoerster R, Dewanjee M. Steady flow in an aneurysm model: correlation between fluid dynamics and blood platelet deposition. J Biomech Eng. 1996; 118:280–286. [PubMed: 8872248]

9. Bluestein D, Niu L, Schoephoerster RT, Dewanjee MK. Fluid mechanics of arterial stenosis: relationship to the development of mural thrombus. Ann Biomed Eng. 1997; 25:344–356. [PubMed: 9084839]
10. Brash, JL., Horbett, TA. I Proteins at Interfaces 'Physicochemicel. 1995.
11. Brown JM, O'Brien SM, Wu C, Sikora JAH, Griffith BP, Gammie JS. Isolated aortic valve replacement in North America comprising 108,687 patients in 10 years: changes in risks, valve types, and outcomes in the Society of Thoracic Surgeons National Database. The Journal of thoracic and cardiovascular surgery. 2009; 137:82–90. [PubMed: 19154908]
12. Bruneau C-H, Mortazavi I. Numerical modelling and passive flow control using porous media. Computers & Fluids. 2008; 37:488–498.
13. Cannegieter S, Rosendaal F, Briet E. Thromboembolic and bleeding complications in patients with mechanical heart valve prostheses. Circulation. 1994; 89:635–641. [PubMed: 8313552]
14. Cassie A, Baxter S. Wettability of porous surfaces. Transactions of the Faraday Society. 1944; 40:546–551.
15. Chang B, Lim S, Kim D, Seo J, Cho S, Shim W, Chung N, Kim S, Cho B. Long-term results with St. Jude Medical and Carbo Medics prosthetic heart valves. The Journal of heart valve disease. 2001; 10:185–194. discussion 195. [PubMed: 11297205]
16. Chiang YP, Chikwe J, Moskowitz AJ, Itagaki S, Adams DH, Egorova NN. Survival and long-term outcomes following bioprosthetic vs mechanical aortic valve replacement in patients aged 50 to 69 years. JAMA. 2014; 312:1323–1329. [PubMed: 25268439]
17. Choi CH, Ulmanella U, Kim J, Ho CM, Kim CJ. Effective slip and friction reduction in nanograted superhydrophobic microchannels. Physics of Fluids (1994-present). 2006; 18:087105.
18. Conn G, Kidane AG, Punshon G, Kannan RY, Hamilton G, Seifalian AM. Is there an alternative to systemic anticoagulation, as related to interventional biomedical devices? Expert Rev Med Devices. 2006; 3:245–261. [PubMed: 16515390]
19. Constantinides P. Plaque fissures in human coronary thrombosis. Journal of Atherosclerosis Research. 1966; 6:1–17.
20. Crawford ST. Pathology of ischaemic heart disease. 1977
21. Crouzet C, Decker C, Marchal J. Characterization of Primary Reactions of Oxidative-Degradation in Course of Autoxidation of Poly (Oxyethlene) S at 25 Degreesc-Study in Aqueous-Solution with Initiation by Irradiation of Solvent. 8. Kinetic Studies at Ph Between 1 and 1. Makromolekulare Chemie-Macromolecular Chemistry and Physics. 1976; 177:145–157.
22. Daebritz SH, Fausten B, Hermanns B, Franke A, Schroeder J, Groetzner J, Autschbach R, Messmer BJ, Sachweh JS. New flexible polymeric heart valve prostheses for the mitral and aortic positions. Heart Surg Forum. 2004:E525–E532.
23. Damodaran VB, Leszczak V, Wold KA, Lantvit SM, Popat KC, Reynolds MM. Antithrombogenic properties of a nitric oxide-releasing dextran derivative: evaluation of platelet activation and whole blood clotting kinetics. RSC advances. 2013; 3:24406–24414.
24. Daniello RJ, Waterhouse NE, Rothstein JP. Drag reduction in turbulent flows over superhydrophobic surfaces. Physics of Fluids (1994-present). 2009; 21:085103.
25. Dasi LP, Ge L, Simon HA, Sotiropoulos F, Yoganathan AP. Vorticity dynamics of a bileaflet mechanical heart valve in an axisymmetric aorta. Physics of Fluids. 2007; 19
26. Dasi LP, Murphy DW, Glezer A, Yoganathan AP. Passive flow control of bileaflet mechanical heart valve leakage flow. J Biomech. 2008; 41:1166–1173. [PubMed: 18374925]
27. De Scheerder I, Wang K, Wilczek K, Meuleman D, Van Amsterdam R, Vogel G, Piessens J, Van de Werf F. Experimental study of thrombogenicity and foreign body reaction induced by heparin-coated coronary stents. Circulation. 1997; 95:1549–1553. [PubMed: 9118524]
28. Dooley PN, Quinlan NJ. Effect of Eddy Length Scale on Mechanical Loading of Blood Cells in Turbulent Flow. Ann Biomed Eng. 2009; 37:2449–2458. [PubMed: 19757062]
29. Dussan VE, Chow RTP. On the ability of drops or bubbles to stick to non-horizontal surfaces of solids. J Fluid Mech. 1983; 137:1–29.
30. Fallon AM, Shah N, Marzec UM, Warnock JN, Yoganathan AP, Hanson SR. Flow and thrombosis at orifices simulating mechanical heart valve leakage regions. J Biomech Eng. 2006; 128:30–39. [PubMed: 16532615]

31. Forleo, M. Mechanical Engineering. Fort Collins: Colorado State University; 2014. Application of passive flow control to mitigate the thromboembolic potential of bileaflet mechanical heart valves : an in-vitro study; p. 193
32. Forleo M, Dasi L. Effect of Hypertension on the Closing Dynamics and Lagrangian Blood Damage Index Measure of the B-Datum Regurgitant Jet in a Bileaflet Mechanical Heart Valve. Ann Biomed Eng. 2013:1–13.
33. Gammie JS, Sheng S, Griffith BP, Peterson ED, Rankin JS, O'Brien SM, Brown JM. Trends in mitral valve surgery in the United States: results from the Society of Thoracic Surgeons Adult Cardiac Database. The Annals of Thoracic Surgery. 2009; 87:1431–1439. [PubMed: 19379881]
34. Ge L, Dasi LP, Sotiropoulos F, Yoganathan AP. Characterization of hemodynamic forces induced by mechanical heart valves: Reynolds vs. viscous stresses. Ann Biomed Eng. 2008; 36:276–297. [PubMed: 18049902]
35. Gerring E, Bellhouse B, Bellhouse F, Haworth W. Long term animal trials of the Oxford aortic/pulmonary valve prosthesis without anticoagulants. ASAIO J. 1974; 20:703–707.
36. Giersiepen M, Wurzinger L, Opitz R, Reul H. Estimation of shear stress-related blood damage in heart valve prostheses--in vitro comparison of 25 aortic valves. The International journal of artificial organs. 1990; 13:300–306. [PubMed: 2365485]
37. Godek M, Michel R, Chamberlain L, Castner D, Grainger D. Adsorbed serum albumin is permissive to macrophage attachment to perfluorocarbon polymer surfaces in culture. Journal of Biomedical Materials Research Part A. 2009; 88:503–519. [PubMed: 18306309]
38. Hellums JD. 1993 Whitaker Lecture: biorheology in thrombosis research. Ann Biomed Eng. 1994; 22:445–455. [PubMed: 7825747]
39. Huang PY, Hellums JD. Aggregation and disaggregation kinetics of human blood platelets: Part II. Shear-induced platelet aggregation. Biophys J. 1993; 65:344–353. [PubMed: 8369442]
40. Ibrahim M, O'Kane H, Cleland J, Gladstone D, Sarsam M, Patterson C. The St. Jude Medical prosthesis. A thirteen-year experience. The Journal of thoracic and cardiovascular surgery. 1994; 108:221–230. [PubMed: 8041170]
41. Jaffer I, Fredenburgh J, Hirsh J, Weitz J. Medical device-induced thrombosis: what causes it and how can we prevent it? J Thromb Haemost. 2015; 13:S72–S81. [PubMed: 26149053]
42. Jordan SW, Haller CA, Sallach RE, Apkarian RP, Hanson SR, Chaikof EL. The effect of a recombinant elastin-mimetic coating of an ePTFE prosthesis on acute thrombogenicity in a baboon arteriovenous shunt. Biomaterials. 2007; 28:1191–1197. [PubMed: 17087991]
43. Kaneko T, Aranki S, Javed Q, McGurk S, Shekar P, Davidson M, Cohn L. Mechanical versus bioprosthetic mitral valve replacement in patients< 65 years old. The Journal of thoracic and cardiovascular surgery. 2014; 147:117–126. [PubMed: 24079878]
44. Kang IK, Kwon BK, Lee JH, Lee HB. Immobilization of proteins on poly (methyl methacrylate) films. Biomaterials. 1993; 14:787–792. [PubMed: 8218730]
45. Khorasani M, Mirzadeh H. In vitro blood compatibility of modified PDMS surfaces as superhydrophobic and superhydrophilic materials. Journal of applied polymer science. 2004; 91:2042–2047.
46. Kota AK, Choi W, Tuteja A. Superomniphobic surfaces: Design and durability. MRS bulletin. 2013; 38:383–390.
47. Kota AK, Mabry JM, Tuteja A. Superoleophobic surfaces: design criteria and recent studies. Surface Innovations. 2013; 1:71–83.
48. Kota AK, Tuteja A. High-efficiency, ultrafast separation of emulsified oil-water mixtures. NPG Asia Mater. 2013; 5:e58.
49. Kutay V, Noyan T, Ozcan S, Melek Y, Ekim H, Yakut C. Biocompatibility of Heparin-Coated Cardiopulmonary Bypass Circuits in Coronary Patients With Left Ventricular Dysfunction Is Superior to PMEA-Coated Circuits. J Card Surg. 2006; 21:572–577. [PubMed: 17073955]
50. Lee C, Kim CJC. Maximizing the giant liquid slip on superhydrophobic microstructures by nanostructuring their sidewalls. Langmuir. 2009; 25:12812–12818. [PubMed: 19610627]
51. Lee JH, Lee HB, Andrade JD. Blood compatibility of polyethylene oxide surfaces. Progress in Polymer Science. 1995; 20:1043–1079.

52. Leitão AF, Gupta S, Silva JP, Reviakine I, Gama M. Hemocompatibility study of a bacterial cellulose/polyvinyl alcohol nanocomposite. Colloids and Surfaces B: Biointerfaces. 2013; 111:493–502. [PubMed: 23880088]
53. Leslie DC, Waterhouse A, Berthet JB, Valentin TM, Watters AL, Jain A, Kim P, Hatton BD, Nedder A, Donovan K. A bioinspired omniphobic surface coating on medical devices prevents thrombosis and biofouling. Nat Biotechnol. 2014
54. Lin J, Howard F, Selby G. Turbulent flow separation control through passive techniques. 1989
55. Lu P, Lai H, Liu J. A reevaluation and discussion on the threshold limit for hemolysis in a turbulent shear flow. J Biomech. 2001; 34:1361–1364. [PubMed: 11522317]
56. Martell MB, Perot JB, Rothstein JP. Direct numerical simulations of turbulent flows over superhydrophobic surfaces. J Fluid Mech. 2009; 620:31–41.
57. Michael KE V, Vernekar N, Keselowsky BG, Meredith JC, Latour RA, García AJ. Adsorption-induced conformational changes in fibronectin due to interactions with well-defined surface chemistries. Langmuir. 2003; 19:8033–8040.
58. Moake JL, Turner NA, Stathopoulos NA, Nolasco L, Hellums JD. Shear-induced platelet aggregation can be mediated by vWF released from platelets, as well as by exogenous large or unusually large vWF multimers, requires adenosine diphosphate, and is resistant to aspirin. Blood. 1988; 71:1366–1374. [PubMed: 3258770]
59. Morshed KN, Bark D Jr, Forleo M, Dasi LP. Theory to Predict Shear Stress on Cells in Turbulent Blood Flow. PLOS ONE. 2014; 9:e105357. [PubMed: 25171175]
60. Mozaffarian D, Benjamin EJ, Go AS, Arnett DK, Blaha MJ, Cushman M, de Ferranti S, Després J-P, Fullerton HJ, Howard VJ, Huffman MD, Judd SE, Kissela BM, Lackland DT, Lichtman JH, Lisabeth LD, Liu S, Mackey RH, Matchar DB, McGuire DK, Mohler ER, Moy CS, Muntner P, Mussolino ME, Nasir K, Neumar RW, Nichol G, Palaniappan L, Pandey DK, Reeves MJ, Rodriguez CJ, Sorlie PD, Stein J, Towfighi A, Turan TN, Virani SS, Willey JZ, Woo D, Yeh RW, Turner MB. Heart Disease and Stroke Statistics–2015 Update: A Report From the American Heart Association. Circulation. 2014
61. Nishino T, Meguro M, Nakamae K, Matsushita M, Ueda Y. The lowest surface free energy based on-CF3 alignment. Langmuir. 1999; 15:4321–4323.
62. Nobili M, Sheriff J, Morbiducci U, Redaelli A, Bluestein D. Platelet activation due to hemodynamic shear stresses: damage accumulation model and comparison to in vitro measurements. ASAIO journal (American Society for Artificial Internal Organs: 1992). 2008; 54:64. [PubMed: 18204318]
63. Ollivier V, Syvannarath V, Gros A, Butt A, Loyau S, Jandrot-Perrus M, Ho-Tin-Noé B. Collagen can selectively trigger a platelet secretory phenotype via glycoprotein VI. PloS one. 2014; 9:e104712. [PubMed: 25116206]
64. Ou J, Perot B, Rothstein JP. Laminar drag reduction in microchannels using ultrahydrophobic surfaces. Physics of Fluids (1994-present). 2004; 16:4635–4643.
65. Ou J, Rothstein JP. Direct velocity measurements of the flow past drag-reducing ultrahydrophobic surfaces. Physics of Fluids (1994-present). 2005; 17:103606.
66. Prawel D, Dean H, Forleo M, Lewis N, Gangwish J, Popat K, Dasi L, James S. Hemocompatibility and Hemodynamics of Novel Hyaluronan–Polyethylene Materials for Flexible Heart Valve Leaflets. Cardiovasc Eng Technol. 2013:1–12.
67. Quéré D. Non-sticking drops. Reports on Progress in Physics. 2005; 68:2495.
68. Reser D, Seifert B, Klein M, Dreizler T, Hasenclever P, Falk V, Starck C. Retrospective analysis of outcome data with regards to the use of Phisio(R)-, Bioline(R)- or Softline(R)-coated cardiopulmonary bypass circuits in cardiac surgery. Perfusion. 2012; 27:530–534. [PubMed: 22864552]
69. Roach P, Farrar D, Perry CC. Interpretation of protein adsorption: surface-induced conformational changes. J Am Chem Soc. 2005; 127:8168–8173. [PubMed: 15926845]
70. Rothstein JP. Slip on superhydrophobic surfaces. Annu Rev Fluid Mech. 2010; 42:89–109.
71. Sade R, Ballenger J, Hohn A, Arrants J, Riopel D, Taylor A. Cardiac valve replacement in children: comparison of tissue with mechanical prostheses. The Journal of thoracic and cardiovascular surgery. 1979; 78:123–127. [PubMed: 571943]

72. Sallam AM, Hwang N. Human red blood cell hemolysis in a turbulent shear flow: contribution of Reynolds shear stresses. Biorheology. 1983; 21:783–797.
73. Serruys PW, Emanuelsson H, Van Der Giessen W, Lunn AC, Kiemeney F, Macaya C, Rutsch W, Heyndrickx G, Suryapranata H, Legrand V. Heparin-Coated Palmaz-Schatz Stents in Human Coronary Arteries Early Outcome of the Benestent-II Pilot Study. Circulation. 1996; 93:412–422. [PubMed: 8565157]
74. Shepherd G, Mohorn P, Yacoub K, May DW. Adverse drug reaction deaths reported in United States vital statistics, 1999–2006. Ann Pharmacother. 2012; 46:169–175. [PubMed: 22253191]
75. Smith BS, Yoriya S, Grissom L, Grimes CA, Popat KC. Hemocompatibility of titania nanotube arrays. Journal of Biomedical Materials Research Part A. 2010; 95:350–360. [PubMed: 20629021]
76. Sotiropoulos F. Fluid Mechanics of Heart Valves and Their Replacements. Annu Rev Fluid Mech. 2015; 48
77. Srinivasan S, Choi W, Park KC, Chhatre SS, Cohen RE, McKinley GH. Drag reduction for viscous laminar flow on spray-coated non-wetting surfaces. Soft Matter. 2013; 9:5691–5702.
78. Stassano P, Di Tommaso L, Monaco M, Iorio F, Pepino P, Spampinato N, Vosa C. Aortic valve replacement: a prospective randomized evaluation of mechanical versus biological valves in patients ages 55 to 70 years. Journal of the American College of Cardiology. 2009; 54:1862–1868. [PubMed: 19892237]
79. Sun JC, Davidson MJ, Lamy A, Eikelboom JW. Antithrombotic management of patients with prosthetic heart valves: current evidence and future trends. The Lancet. 2009; 374:565–576.
80. Sun T, Tan H, Han D, Fu Q, Jiang L. No platelet can adhere - largely improved blood compatibility on nanostructured superhydrophobic surfaces. Small. 2005; 1:959–963. [PubMed: 17193377]
81. Vongpatanasin W, Hillis LD, Lange RA. Prosthetic heart valves. N Engl J Med. 1996; 335:407–416. [PubMed: 8676934]
82. Vrolix MC V, Legrand M, Reiber JH, Grollier G, Schalij MJ, Brunel P, Martinez-Elbal L, Gomez-Recio M, Bär FW, Bertrand ME. Heparin-coated Wiktor stents in human coronary arteries (MENTOR trial). Am J Cardiol. 2000; 86:385–389. [PubMed: 10946029]
83. Wenzel RN. Resistance of solid surfaces to wetting by water. Industrial & Engineering Chemistry. 1936; 28:988–994.
84. Wheatley D, Bernacca G, Tolland M, O'Connor B, Fisher J, Williams D. Hydrodynamic function of a biostable polyurethane flexible heart valve after six months in sheep. The International journal of artificial organs. 2001; 24:95–101. [PubMed: 11256515]
85. Wisman C, Pierce W, Donachy J, Pae W, Myers J, Prophet G. A polyurethane trileaflet cardiac valve prosthesis: in vitro and in vivo studies. ASAIO J. 1982; 28:164–168.
86. Yacoub M, Halim M, Radley-Smith R, McKay R, Nijveld A, Towers M. Surgical treatment of mitral regurgitation caused by floppy valves: repair versus replacement. Circulation. 1981; 64:II210–216. [PubMed: 7249325]
87. Yoganathan AP, He Z, Casey Jones S. Fluid Mechanics of Heart Valves. Annu Rev Biomed Eng. 2004; 6:331–362. [PubMed: 15255773]
88. Yoganathan, AP., Lemmon, JD., Ellis, JT. Biomedical Engineering Fundamentals. CRC Press; 2006. Heart Valve Dynamics; p. 55-51-55-16.
89. Young T. An Essay on the Cohesion of Fluids. Philosophical Transactions of the Royal Society of London. 1805; 95:65–87.
90. Zhang, J-n, Bergeron, AL., Yu, Q., Sun, C., McIntire, LV., López, JA., Dong, J-f. Platelet aggregation and activation under complex patterns of shear stress. Thrombosis and haemostasis. 2002; 88:817–821. [PubMed: 12428100]

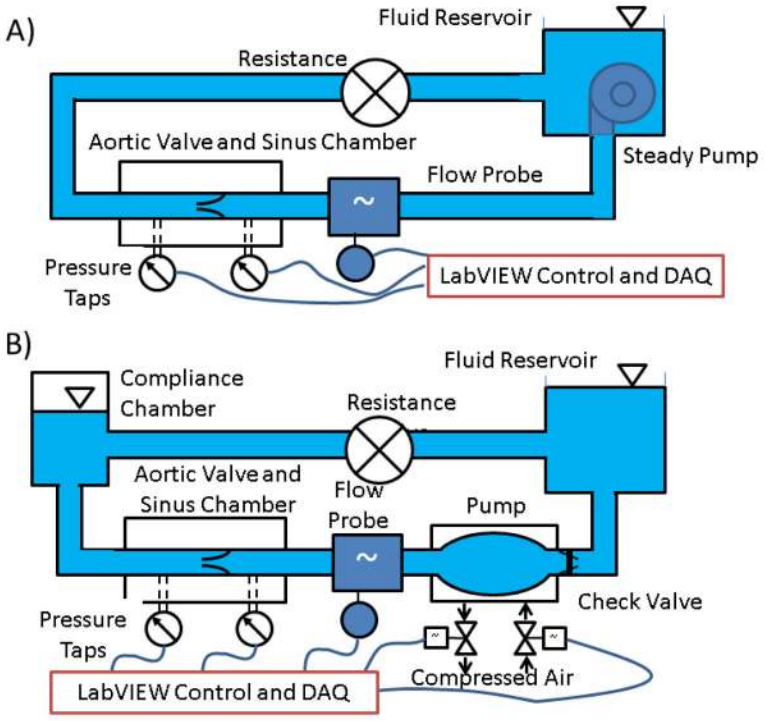


**Figure 1.**
Schematic of steady flow chamber (A) and pulsatile flow chamber (B) with components labeled.

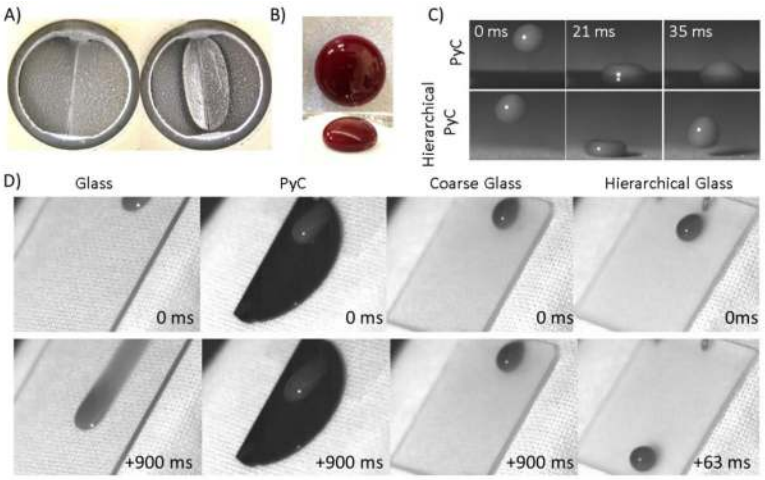


**Figure 2.**

Water (A) and whole blood (B) on a St. Jude Medical bileaflet mechanical heart valve with a dual coating. C) Whole blood droplet falling/bouncing on a pyrolytic carbon (PyC) leaflet and a PyC leaflet with a hierarchical coating (coarse) from a height of 10 mm. D) Blood sliding/rolling on glass, PyC, coarsely coated glass, and glass with the hierarchical coating at a 45º angle for a 30 μl droplet.

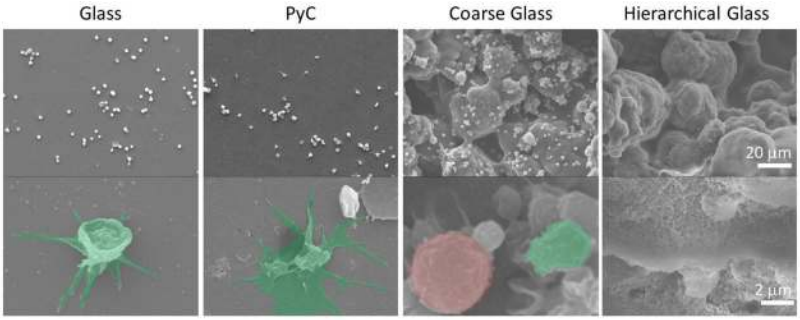


**Figure 3.**

Scanning electron microscope images of glass, PyC, glass with a coarse coating, and glass with a hierarchical coating. Platelet (green) and leukocyte (red) adhesion on various surface treatments. The bottom row is magnified by a factor of 10 more than the top row.

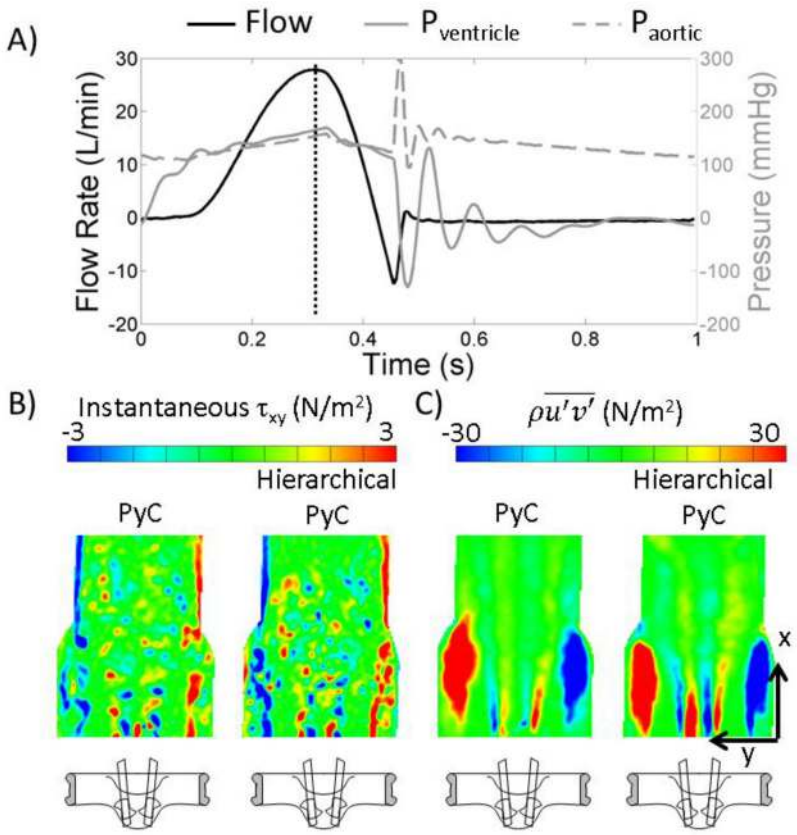


**Figure 4.**

A) Flow rate, ventricular pressure, and aortic pressure ensemble averaged over 5 cycles. A dotted line denotes peak flow, corresponding to the contour plots. B) Instantaneous shear stress contours for ensemble averaged data over 250 cycles downstream of the PyC bileaflet mechanical heart valve (BMHV) and the hierarchical coated PyC BMHV. C) Reynolds shear stress contours for the BMHV and the coated BMHV.

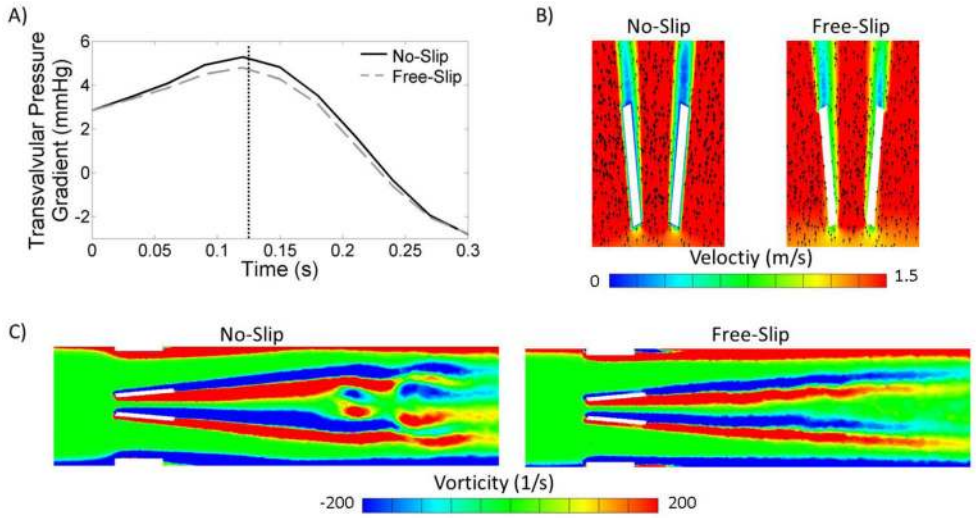


**Figure 5.**

A) Computed transvalvular pressure difference for leaflets with a no-slip and leaflets with a slip condition for a sinusoidal flow input. A dotted line corresponds to the time for the vorticity contour plots. B) Velocity magnitude contours during peak flow illustrating the effects of slip on velocity distribution and its gradients around the leaflets. C) Vorticity contours during flow deceleration for a leaflet boundary layer with a no-slip and a slip condition.

**Table 1**

Contact and roll off angles

| | Glass | PyC | Glass Coarse | Glass Hierarchical |
|---|---|---|---|---|
| Advancing | 49±3° | 70±3° | 116±3° | 164±3° |
| Receding | 15±3° | 47±3° | 70±3° | 160±3° |
| Roll-off | NA | NA | NA | 5±1° |